BASIC RESEARCH

Paradoxical effects of brain death and associated trauma on rat mesenteric microcirculation: an intravital microscopic study

Rafael Simas, Paulina Sannomiya, José Walber M. C. Cruz, Cristiano de Jesus Correia, Fernando Luiz Zanoni, Maurício Kase, Laura Menegat, Isaac Azevedo Silva, Luiz Felipe P. Moreira

Faculdade de Medicina da Universidade de São Paulo, Instituto do Coração (InCor), Laboratório de Cirurgia Cardiovascular e Fisiopatologia da Circulação, São Paulo/SP, Brazil.

OBJECTIVE: Experimental findings support clinical evidence that brain death impairs the viability of organs for transplantation, triggering hemodynamic, hormonal, and inflammatory responses. However, several of these events could be consequences of brain death–associated trauma. This study investigated microcirculatory alterations and systemic inflammatory markers in brain-dead rats and the influence of the associated trauma.

METHOD: Brain death was induced using intracranial balloon inflation; sham-operated rats were trepanned only. After 30 or 180 min, the mesenteric microcirculation was observed using intravital microscopy. The expression of P-selectin and ICAM-1 on the endothelium was evaluated using immunohistochemistry. The serum cytokine, chemokine, and corticosterone levels were quantified using enzyme-linked immunosorbent assays. White blood cell counts were also determined.

RESULTS: Brain death resulted in a decrease in the mesenteric perfusion to 30%, a 2.6-fold increase in the expression of ICAM-1 and leukocyte migration at the mesentery, a 70% reduction in the serum corticosterone level and pronounced leukopenia. Similar increases in the cytokine and chemokine levels were seen in the both the experimental and control animals.

CONCLUSION: The data presented in this study suggest that brain death itself induces hypoperfusion in the mesenteric microcirculation that is associated with a pronounced reduction in the endogenous corticosterone level, thereby leading to increased local inflammation and organ dysfunction. These events are paradoxically associated with induced leukopenia after brain damage.

KEYWORDS: Brain death; inflammation; Intravital microscopy; Mesenteric microcirculation.

INTRODUCTION

In most cases, organs for transplantation come from brain-dead donors, which, by itself, interferes with the viability of the donated organ(s) (1). Brain death (BD) triggers a series of hemodynamic, hormonal, and inflammatory effects that have different roles in the organs that may be transplanted (2). The systemic effects of BD include increased expression of adhesion molecules, increased leukocyte infiltration of different organs, and increased serum cytokine levels (1-3). However, it is unclear which of these events are consequences of BD and which arise from the inflammatory processes triggered by the associated trauma. It is known that brain damage, such as stroke, can induce immunodeficiency, thereby increasing the patient's susceptibility to infection (4). This study aims to characterize the evolution of the inflammatory process in brain-dead rats via intravital microscopy of the mesenteric microcirculation and analysis of systemic markers and to compare the results with those obtained from sham-operated animals followed over time.

MATERIALS AND METHODS

Animal model

Male Wistar rats weighing 250–350 g were used and randomized into four groups: SH30 and SH180, animals operated on without BD induction that were monitored for 30 ($n = 14$) or 180 minutes ($n = 15$), respectively; and BD30 and BD180, which were animals in which BD was induced

and that were monitored for 30 ($n = 17$) or 180 minutes ($n = 15$), respectively. The animals were evaluated at 30 minutes to determine which features were triggered by the BD itself and at 180 min to follow the evolution of the processes. The experimental protocols were approved by the Animal Subject Committee of the Heart Institute (InCor) of the Faculdade de Medicina da Universidade de São Paulo.

Rats were anesthetized in a chamber with 5% isoflurane, intubated, and ventilated with a rodent ventilator (Harvard Apparatus, Holliston, MA, USA) with a tidal volume of 10 ml/kg and a frequency of 70 breaths/min. Sedation of the animals was maintained via continual inhalation of 2% isoflurane. The carotid artery was cannulated for continuous blood pressure monitoring and blood sampling. The jugular vein was cannulated for infusion of saline solution.

Brain death model

A Fogarty-4F catheter (Baxter Health Care, Deerfield, IL, USA) was placed into the intracranial cavity of rats in the BD groups through a drilled parietal burr hole. The balloon catheter was rapidly inflated with 0.5 ml of saline, and the intracranial pressure increased until BD was confirmed via maximal pupil dilatation, apnea, an absence of reflexes, and a drop of the mean arterial pressure (MAP). Anesthesia was stopped after the induction of BD. In the sham group, animals underwent surgery, and the trepanation was performed, but the catheter was not placed into the intracranial cavity. Anesthesia was maintained throughout the experiment for the animals in the sham groups. Brain-dead rats received an infusion of saline solution (2 ml/h) through the jugular vein to minimize dehydration.

Blood gases, electrolyte and lactate levels, hematocrit, and white blood cell counts

Blood gases and electrolyte and lactate levels were measured using blood samples obtained from the carotid artery at baseline (0 min) and 30 or 180 min after the surgical procedures using a gas analyzer (Radiometer ABL 555, Radiometer Medical, Copenhagen, Denmark). The hematocrit and white blood cell counts were determined using blood samples obtained from the cut tip of the tail vein at the same time points. The hematocrit was measured using microcapillary tube centrifugation. Total white blood cell counts were determined using a Neubauer chamber. Differential cell counts were performed on stained films that were visualized using oil immersion microscopy. A total of 100 cells were counted and classified on the basis of normal morphological criteria.

Intravital microcopy of the mesenteric microcirculation

Intravital microscopy of the mesenteric microcirculation was performed as previously described (5). After 30 or 180 minutes, an abdominal midline incision was performed, and the distal ileum and its accompanying mesentery were exposed for *in vivo* microscopic examination of the microcirculation. The animals were maintained on a specially designed stage warmed with circulating water maintained at 37℃. The stage had a transparent platform on which the tissue to be transilluminated was placed. The mesentery was continuously perfused throughout the study period with a warmed (37℃) Krebs-Henseleit solution (113 mmol/l NaCl,

4.7 mmol/l KCl, 2.5 mmol/l $CaCl_2 \cdot 2H_2O$, 25 mmol/l $NaHCO_3$, 1.1 mmol/l $MgSO_4$, 1.1 mmol/l KH_2PO_4, 5 mmol/l glucose, pH 7.2–7.4) that was saturated with a mixture of gases (95% N_2 and 5% CO_2). A color camera (AxioCam HSc, Carl Zeiss, München-Hallbergmos, Germany) was coupled onto a triocular microscope (Axioplan 2, Carl Zeiss), and the microcirculatory variables were analyzed using the Axiovision 4.1 imaging software (Carl Zeiss). The vascular density was analyzed using a $10\times$ light microscopic objective and a 1 mm^2 area on the computer screen. The type of flow was defined as continuous or intermittent/absent. Vessels were separated into large and small vessels using a cutoff diameter value of 30 μm. Five fields were selected for each animal. To evaluate leukocyte-endothelial interactions, three post-capillary venules, with diameters ranging from 15 to 25 μm, were selected for each animal. The number of rolling leukocytes is presented as the mean number of white blood cells passing a designated line perpendicular to the venular axis per 10 min. The rolling velocity in each vessel was determined as the average velocity of 10 leukocytes that traveled a defined distance in the microvessel. Adherent cells (i.e., leukocytes that remained stationary for more than 30 seconds on the venular endothelium) were counted during a 10-min period in a 100-μm segment of the vessel. The number of leukocytes accumulating in the connective tissue adjacent to the chosen post-capillary venule was determined in a standard area of 5,000 μm^2.

Immunohistochemistry for P-selectin and ICAM-1

Animals were exsanguinated from the abdominal aorta, and the mesentery was removed, immersed in hexane, and frozen with liquid nitrogen. Serial slices of the mesentery (8 μm) were placed onto glass slides, which were previously coated with organosilane (Sigma Chemical Co, St. Louis, MO, USA). The samples were fixed in acetone for the immunodetection of both intercellular adhesion molecule (ICAM)-1 and P-Selectin on the mesenteric microvessels. SuperBlock buffer (Pierce Biotechnology, Rockford, IL, USA) was used to block non-specific sites. The tissue sections were incubated overnight at 4℃ with a biotin-conjugated anti-rat ICAM-1 (CD54) monoclonal antibody (Seikagaku, Tokyo, Japan) or a biotin-conjugated anti-P-selectin monoclonal antibody (CD62P, R&D System, Minneapolis, MN, USA). Both antibodies were diluted 1:50 in phosphate-buffered saline (PBS) containing 0.3% Tween 20. After washing the slides with PBS, the sections were incubated for 1 h at room temperature with streptavidin-conjugated fluorescein (Amersham Pharmacia Biotech, London, UK) diluted 1:200. After washing the slides with PBS, the samples were treated with Vectashield mounting medium containing propidium iodide (Vector, Burlingame, CA, USA) to preserve the fluorescence. Negative-control samples were incubated with PBS instead of the primary antibody. The system used for image acquisition included a CoolSNAP-Pro Color digital camera (Nikon, Tokyo, Japan) coupled to a triocular fluorescence microscope (Nikon). All images were acquired using Image-Pro Plus software, version 4.1 (Media Cybernetics, Silver Spring, MD, USA). The results are presented as the mean fluorescence intensity.

Serum concentrations of cytokines, chemokines and corticosterone

Blood samples were obtained from the carotid artery of brain-dead rats and sham-treated rats 30 or 180 minutes after the surgical procedures were performed. After

centrifugation ($1500 \times g$, $25°C$), the serum concentration of tumor necrosis factor (TNF)-α, interleukin (IL)-1β, IL-6, IL-10, cytokine-induced neutrophil chemoattractant (CINC)-1, CINC-2 (R&D Systems, Minneapolis, MN, USA), and corticosterone (Cayman Chemical, Ann Arbor, MI, USA) was determined using enzyme-linked immunosorbent assays (ELISA), as recommended by the manufacturer.

Statistical analysis

All data are presented as the mean $\pm$ standard error of the mean (SEM). The overall group differences were compared using a multivariate general linear model with group and time as the factors with a *post hoc* Bonferroni test. A *p*-value of less than 0.05 was considered to be significant. All statistical analyses were performed using SPSS for Windows, version 17.0 (SPSS, Chicago, IL, USA).

RESULTS

Hemodynamic parameters, arterial blood gases, electrolyte and lactate levels, and hematocrits

The induction of BD was associated with a sudden increase in the MAP over the first minute following catheter inflation. This increase was followed by a decrease in the MAP below the baseline level and a subsequent increase to a normal level after one hour. In the SH rats, no differences were observed in the MAP over time (Figure 1). There were no differences in the heart rate between the groups. No differences were observed in the arterial blood gases and electrolyte, lactate and hematocrit values between the BD and SH groups at baseline, 30 min, and 180 min after the surgical procedures (data not shown).

Mesenteric microcirculatory variables

Microvascular perfusion was evaluated 30 and 180 min after brain death. There was a prompt interruption in the perfusion of mesenteric microvessels measuring less than 30 μm in diameter. The average proportion of perfused small vessels in BD rats was 30% compared to 76% in SH rats. The results are summarized in Table 1. Representative photomicrographs of mesenteric microvessels are shown in Figure 2. To evaluate leukocyte-endothelial interactions in the perfused small vessels, the rolling leukocyte velocity and the number of rolling, adhered and migrated cells were determined 30 and 180 min after the surgical procedures. There were no differences in the rolling leukocyte velocity between BD and SH rats after 30 or 180 min. However, the number of rolling leukocytes in BD rats was significantly reduced 30 min (50%) and 180 min (73%) after surgery compared with the number in SH rats (Table 1). The adhesion of leukocytes to the endothelium was significantly reduced in BD rats only after 180 min. However, despite this reduction, BD rats exhibited an increased number of migrated cells compared with SH rats. This result was accompanied by a pronounced leukopenia, as demonstrated by the blood leukocyte count in BD rats after 180 min. Compared with the 30-min time point, the neutrophil/lymphocyte ratio was significantly increased in both the BD and SH groups at 180 min.

Expression of P-selectin and ICAM-1

As seen in Figure 3A, the expression of P-selectin on the mesenteric microvessels increased above the baseline reference values at 30 min and 180 min; no differences in the expression levels were seen comparing BD and SH rats. In contrast, ICAM-1 expression in the microvessels was significantly increased (2.6-fold) in BD rats compared with SH rats at the 180-min time point (Figure 3C). Representative photomicrographs of the staining for P-selectin and ICAM-1 on the mesenteric microvessels of BD and SH rats are shown in Figures 3B and 3D.

Serum cytokine and chemokine levels

Similar increases were observed in the serum concentrations of TNF-α, IL-1β, IL-6, IL-10, CINC-1, and CINC-2 in
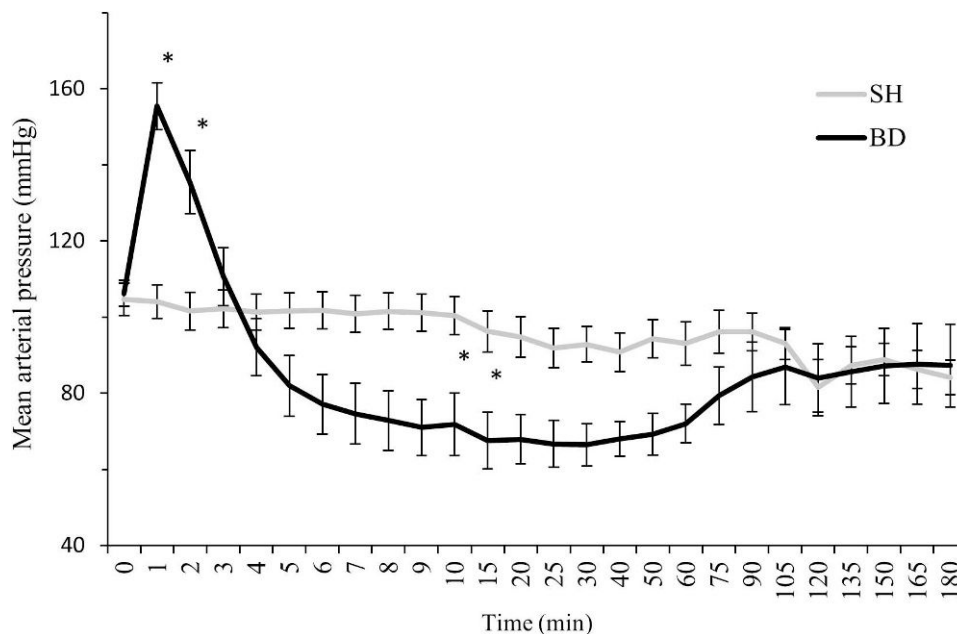

Figure 1 - Mean arterial pressure of brain-dead (BD, $n = 12$) and sham-operated (SH, $n = 12$) rats 180 minutes after the surgical procedure. The animals were monitored over time. The data are presented as the mean $\pm$ SEM. *$p < 0.05$ vs. SH.

Table 1 - Intravital microscopy of the rat mesenteric microcirculation.

	BD30	SH30	BD180	SH180	p_{ANOVA}
Perfused Small Vessels (%)	30.2±0.06‡	77.9±0.07	27.9±0.07‡	74.3±0.06	<0.0001
Rolling Leukocytes (10 min)	89±8*	178±24	87±8†	329±24	<0.0001
Rolling Leukocyte Velocity (µm/s)	22.4±2.2	25.9±3.4	33.5±4.6	40.2±8.3	0.40
Adhered Leukocytes (100 µm venule length)	2.2±0.3	2.2±0.5	3.7±1.0*	7.5±0.5	0.06
Migrated Leukocytes (5,000 µm²)	0.6±0.1	0.6±0.3	2.3±0.3**	1.3±0.3	0.03
Blood Leukocyte Count (mm³)	6.150±459	8.950±1.074	8.157±866*	11.771±1.122	0.01
Neutrophil/Lymphocyte Ratio	0.17±0.02	0.54±0.17	1.77±0.37#	2.31±0.36§	<0.0001

Brain-dead (BD) and sham-operated (SH) rats were analyzed 30 and 180 minutes after the surgical procedures. The data are presented as the mean±SEM for 8–12 rats/group.
*$p<0.05$
**$p<0.01$
†$p<0.001$
‡$p<0.0001$, comparing the BD and SH groups at the same time point.
#$p<0.05$ vs. BD30.
§$p<0.01$ vs. SH30.

both the BD and SH groups at 30 min and 180 min after the surgical procedures. The reference values obtained from normal rats were below the limit of detection for the assay. The results are summarized in Table 2.

Serum corticosterone level

Both BD and SH rats exhibited similar increases in the serum corticosterone level at the 30-min time point, as observed in Figure 4. In contrast, the serum corticosterone level in BD rats was reduced to 30% of the value seen in SH rats at the 180-min time point.

DISCUSSION

Numerous studies have been performed to evaluate the role of BD in graft outcomes in both experimental and clinical studies. In acute evaluations of human BD, catecholamine levels were above normal values immediately after the BD event and remained higher after several hours, with increased inflammatory responses and apoptosis being observed in different organ samples (1,6,7). In a rodent model of heart transplantation, a longer duration of BD leads to increased leukocyte infiltration and expression

of adhesion molecules on the endothelial cells of the transplanted graft, thereby resulting in accelerated acute rejection (8). Experimental studies performed in rats also show that prolonged periods of BD result in more extensive damage to the kidneys (9).

The data presented in this study indicate that BD induces an immediate organ hypoperfusion and an increase in the local inflammatory response that is associated with a reduction in the serum corticosterone level and leukopenia. Some of the observed inflammatory events are triggered by BD-associated trauma.

Such factors as polytrauma, hypoxia, and intracranial bleeding can influence the course of the inflammatory process triggered by BD in different organs (1,2). To evaluate the role of BD-associated trauma, matching sham-operated rats were assessed over time. As described previously, BD leads to an increase in the MAP followed by hypotension (6,10), both of which compromise organ perfusion (11). Our study demonstrates that BD-associated trauma did not influence hemodynamic and perfusion parameters, suggesting that all of the observed changes in MAP and mesenteric hypoperfusion were triggered by the BD itself.
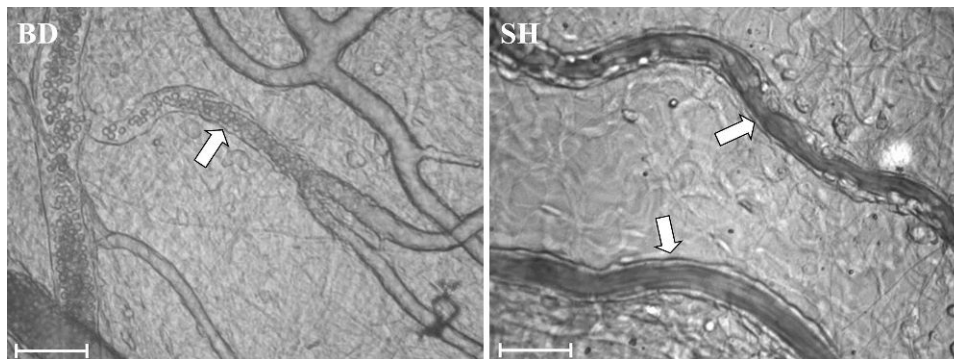

Figure 2 - Photomicrographs of rat mesenteric microvessels. The arrows indicate post-capillary venules in brain-dead (BD) and sham-operated (SH) animals. Bar = 50 µm.
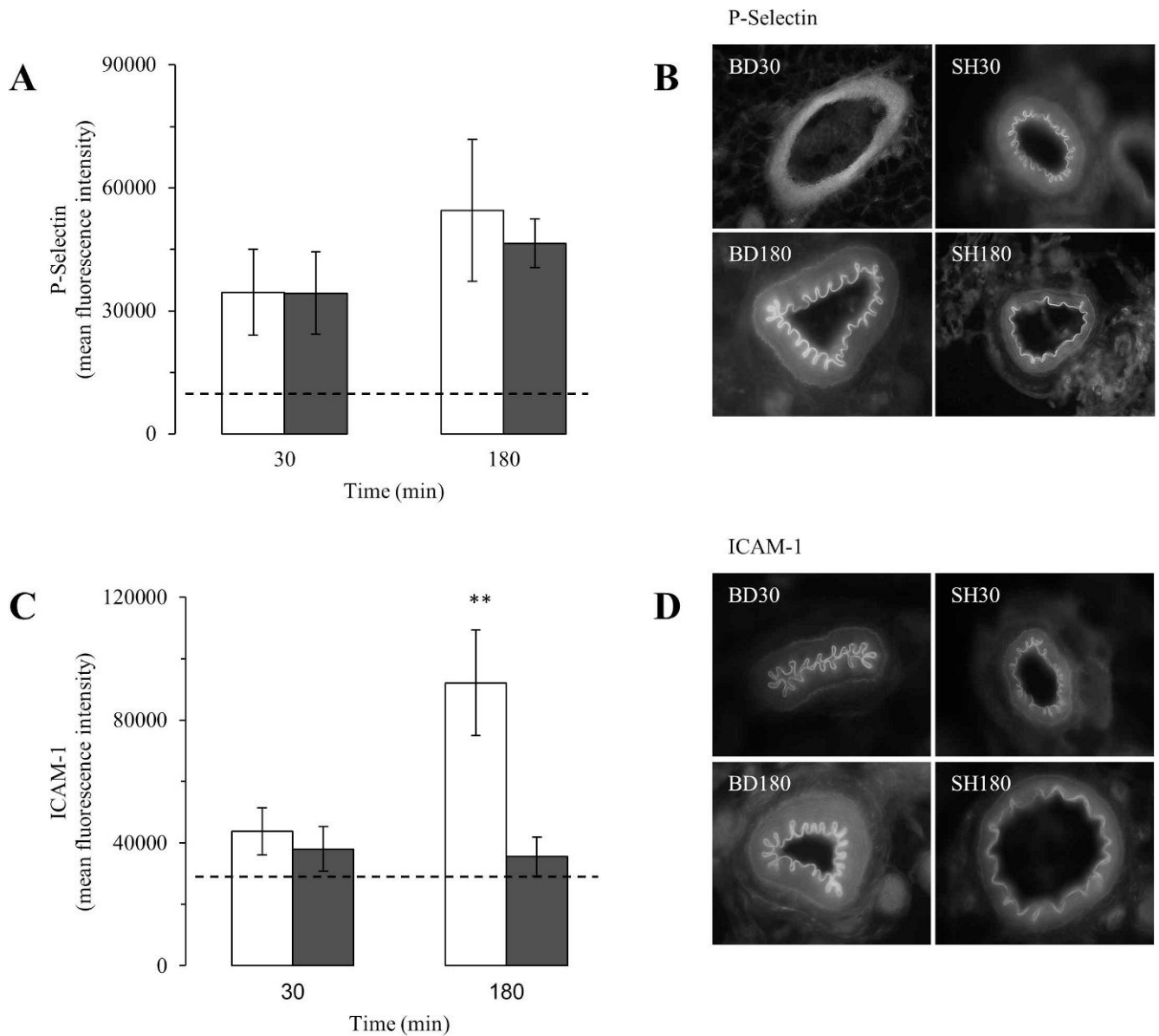
P-Selectin

ICAM-1

Figure 3 - Expression levels of P-selectin (A and B) and ICAM-1 (C and D) in the mesenteric microvessels in brain-dead (BD, white columns) and sham-operated (SH, gray columns) rats 30 and 180 min after the surgical procedure. The values are presented as the mean $\pm$ SEM for nine samples/rat, three rats/group. The dashed lines indicate the basal values. ANOVA P-selectin $p = 0.43$; ICAM-1 $p = 0.003$. ** $p < 0.01$ vs. SH at the same time point.

Intravital microscopy has been used to assess microcirculation in experimental models, but few studies have used this technique following BD (11,12). In this study, intravital microscopy was used to evaluate mesenteric perfusion and leukocyte-endothelial interactions in post-capillary venules of BD and SH rats.

Table 2 - Enzyme-linked immunosorbent assay of serum cytokines and chemokines.

	SH30	BD30	SH180	BD180	p_{ANOVA}
TNF-α (pg/mL)	114.5 ± 22.5	152.3 ± 36.5	48.7 ± 12.2	46.6 ± 13.4	0.45
IL-1β (pg/mL)	240.7 ± 21.7	252.4 ± 22.8	232.4 ± 19.5	256.5 ± 22.0	0.41
IL-6 (pg/mL)	165.3 ± 17.3	239.9 ± 39.5	272.3 ± 55.8	295.6 ± 61.9	0.29
IL-10 (pg/mL)	717.6 ± 87.9	914.9 ± 69.4	350.7 ± 22.7	338.8 ± 42.1	0.12
CINC-1 (pg/mL)	430.0 ± 95.5	519.8 ± 87.4	408.1 ± 70.8	496.2 ± 48.9	0.25
CINC-2 (pg/mL)	62.3 ± 15.6	51.2 ± 7.9	54.4 ± 8.1	88.3 ± 27.6	0.49

Brain-dead (BD) and sham-operated (SH) rats were evaluated 30 and 180 min after the surgical procedures. The data are presented as the mean $\pm$ SEM for 10 rats/group. The reference values obtained from normal rats were below the limit of detection for the assay.
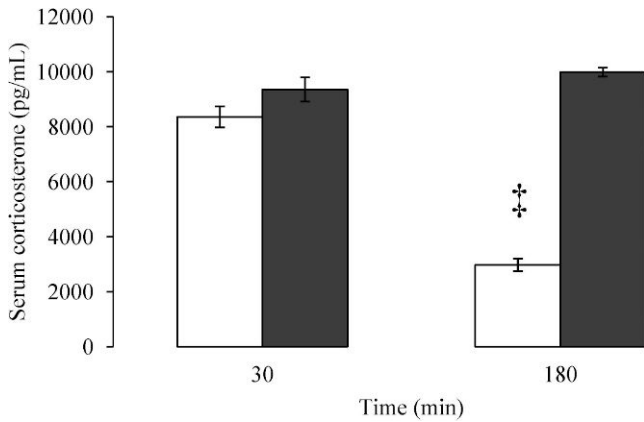
Figure 4 - Enzyme-linked immunosorbent assay for the serum corticosterone level in brain-dead (white columns) and sham-operated (gray columns) rats 30 and 180 minutes after the surgical procedure. The data are presented as the mean $\pm$ SEM for 10 rats/group. ANOVA $p < 0.0001$. ‡$p < 0.0001$ vs. SH at the same time point.

These data indicate that the proportion of perfused small vessels (< 30 μm diameter) was promptly reduced to 30% in the BD rats, whereas perfusion was maintained in the SH rats. As both groups of animals were trepanned, this result suggests that the hypoperfusion of the mesenteric microcirculation was triggered by the BD itself. Decreased organ perfusion following BD has been previously demonstrated. Obermeier et al. (11) described a decrease in the functional capillary density in the pancreatic microcirculation after BD induction in rats using intravital epifluorescence microscopy. In another study, BD induced the deterioration of the rat hepatic microcirculation, including a reduced sinusoidal perfusion rate and sinusoidal diameter (13).

It has been demonstrated that decreased organ perfusion and a progressive inflammatory activation of endothelial cells and leukocytes are observed after BD (9,14-16). In this study, BD rats exhibited a decreased number of rolling leukocytes in the mesenteric microvessels compared to SH rats; however, this reduction was unrelated to the velocity of rolling leukocytes. Both groups of animals presented increases in the number of adherent and migrated leukocytes over time and increased neutrophil/lymphocyte ratios, despite the fact that leukopenia is present in BD rats. In contrast, relative to SH rats, the migration of leukocytes to the perivascular tissue was significantly increased in BD rats after 3 h. These experimental findings agree with the clinical evidence demonstrating that cerebral injury not only leads to brain tissue damage and subsequent local inflammation but also to alterations of the peripheral immune system. It has been demonstrated that stroke induces a rapid lymphocytopenia that is attributed to the apoptosis resulting from the storm of catecholamines and steroids that are immediately released after cerebral ischemia (4,17).

Specific adhesion glycoproteins expressed on the surfaces of leukocytes and endothelial cells play important roles in leukocyte accumulation in a tissue (11,12). Members of the selectin family of cell adhesion molecules are thought to mediate leukocyte rolling along the walls of the microvasculature (18,19). Glycoproteins in the CD11/CD18 complex (β_2-integrins) expressed on leukocytes interact with ligands, such as ICAM-1, on endothelial cells to mediate leukocyte adhesion and emigration (20,21). It has been shown that BD enhances the expression of P-selectin (13). and ICAM-1 in the liver (13-15), kidney (9), and lungs (16). The data presented here demonstrated that the expression of P-selectin on mesenteric microvessels increased at 30 min with no further increase at the 180-min time point. However, there were no significant differences between the BD and SH rats. In contrast, ICAM-1 was upregulated in BD rats at 180 min compared to SH rats, indicating that it was responsible for the leukocyte migration to the perivascular tissue.

The capacity of leukocytes to interact with the endothelium depends on the activation of endothelial cells by cytokines, such as TNF-α and IL-1β. This activation results in the upregulation or de novo synthesis of a variety of chemokines and adhesion molecules, including ICAM-1 (22,23). Studies investigating the relationship between BD and the activation of peripheral organs have demonstrated that cytokines act as signaling molecules during the inflammatory process (1). However, the data presented in this study demonstrates that similar increases in the systemic levels of cytokines (e.g., TNF-α, IL-1β, IL-6, and IL-10) and chemokines (e.g., CINC-1 and -2, analogs of the IL-8 family in humans) were observed in both BD and SH rats.

The host response to inflammation is the result of several processes that occur both locally at the site of injury and systemically. Whereas some parameters of the inflammatory process triggered by BD, including cytokine release, expression of the endothelial adhesion molecule P-selectin and mobilization of neutrophils, were present in the BD and SH rats in this study, the expression of ICAM-1 and neutrophil migration increased in the BD rats only. It is known that BD impairs the endocrine system and decreases the release of hormones, such as triiodothyronine (T3), thyroxine (T4), cortisol, and antidiuretic hormone, thereby suggesting an interruption along the hypothalamic-pituitary-adrenal axis (24,25). Interactions among the central nervous system, the hypothalamic-pituitary-adrenal axis, and components of the innate and adaptive immune system play key roles in the regulation of inflammation (26). Endogenous glucocorticoids, which are secreted in larger amounts at the early stages of an inflammatory reaction, are thought to regulate the initiation and subsequent course of the inflammatory reaction (27). The functions of almost all cellular components of the microcirculation associated with an inflammatory response, including vascular permeability, adhesion molecule expression, and leukocyte extravasation, are affected by glucocorticoids (28). In this regard, the increased levels of ICAM-1 on the mesenteric microvessels of BD rats were associated with a pronounced reduction in the serum corticosterone level. Indeed, dexamethasone reduces the IL-1β-induced expression of ICAM-1 in the rat mesenteric microvascular bed (29). In addition, the treatment of mice with dexamethasone abolished ICAM-1 induction in intestinal vascular beds during endotoxemia (30).

In conclusion, the data presented in this study suggest that BD itself induces hypoperfusion of the mesenteric microcirculation that is associated with a pronounced reduction in the endogenous corticosterone level, thereby leading to increased local inflammation and organ dysfunction. These events are paradoxically associated with induced leukopenia after brain damage. These data need

to be investigated through further studies, including longer observation times after BD induction.

AUTHOR CONTRIBUTIONS

Simas R performed the study and wrote the paper. Sannomiya P analyzed the data and wrote the paper. Cruz JWMC provided support with the intravital microscopy and immunohistochemistry. Correia CJ provided surgical support. Zanoni FL provided support with the enzyme-linked immunosorbent assays. Kase M provided support with the immunohistochemistry. Menegat L provided support with the white blood cell count determination. Silva IA wrote the paper. Moreira LFP analyzed the data and wrote the paper.

REFERENCES

1. Barklin A. Systemic inflammation in the brain-dead organ donor. Acta Anaesthesiol Scand. 2009;53:425-35, doi: 10.1111/j.1399-6576.2008.01879.x.

2. Domínguez-Roldán JM, García-Alfaro C, Jimenéz-González PI, Hernández-Hazañas F, Castillo MLG, Guerrero JJE. Brain death: repercussion on the organs and tissues. Med Intensiva. 2009;33:434-41, doi: 10.1016/j.medin.2009.03.008.

3. Catania A, Lonatti C, Sordi A, Gatti S. Detrimental consequences of brain injury on peripheral cells. Brain Behav Immun. 2009;23:877-84, doi: 10.1016/j.bbi.2009.04.006.

4. Prass K, Meisel C, Höflich C, Braun J, Halle E, Wolf T, et al. Stroke-induced immunodeficiency promotes spontaneous bacterial infection and is mediated by sympathetic activation reversal by poststroke T helper cell type 1-like immunostimulation. J Exp Med. 2003;198:725-36, doi: 10.1084/jem.20021098.

5. Nakagawa NK, Nogueira RA, Correia CJ, Shiwa SR, Cruz JWC, Poli de Figueiredo LF, et al. Leukocyte-endothelium interactions after hemorrhagic shock/reperfusion and cecal ligation/puncture: an intravital microscopic study in rat mesentery. Shock. 2006;26:180-6, doi: 10.1097/01.shk.0000223133.10254.82

6. Barklin A, Larsson A, Vestergaard C, Koefoed-Nielsen J, Bach A, Nyboe R, et al. Does brain death induce a pro-inflammatory response at the organ level in a porcine model? Acta Anaesthesiol Scand. 2008;52:621-7, doi: 10.1111/j.1399-6576.2008.01607.x.

7. López SP, Hernández JO, Moreno NV, Augusto ED, Menéndez FA, González AA. Brain Death Effects on Catecholamine Levels and Subsequent Cardiac Damage Assessed in Organ Donors. J Heart Lung Transplant. 2009;28:815-20, doi: 10.1016/j.healun.2009.04.021.

8. Wilhelm MJ, Pratschke J, Beato F, Taal M, Kusaka M, Hancock WW, et al. Activation of the heart by donor brain death accelerates acute rejection after transplantation. Circulation. 2000;102:2426-33, doi: 10.1161/01.CIR.102.19.2426.

9. van der Hoeven JA, Molema G, Ter Horst GJ, Freund RL, Wiersema J, van Schilfgaarde R, et al. Relationship between duration of brain death and hemodynamic (in)stability on progressive dysfunction and increased immunologic activation of donor kidneys. Kidney Int. 2003;64:1874-82, doi: 10.1046/j.1523-1755.2003.00272.x.

10. Rostron AJ, Avlonitis VS, Cork DMW, Grenade DS, Kirby JA, Dark JH. Hemodynamic resuscitation with arginine vasopressin reduces lung injury after brain death in the transplant donor. Transplantation. 2008;85:597-606, doi: 10.1097/TP.0b013e31816398dd.

11. Obermaier R, von Dobschuetz E, Keck T, Hopp HH, Drognitz O, Schareck W, et al. Brain death impairs pancreatic microcirculation. Am J Transplant. 2004;4:210-5, doi: 10.1046/j.1600-6143.2003.00317.x.

12. Ley K, Laudanna C, Cybulsky MI, Nourshargh S. Getting to the site of inflammation: the leukocyte adhesion cascade update. Nat Rev Immunol. 2007;7:678-89, doi: 10.1038/nri2156.

13. Yamagami K, Hutter J, Yamamoto Y, Schauer RJ, Enders G, Leiderer R, et al. Synergistic effects of brain death and liver steatosis on the hepatic microcirculation. Transplant. 2005;80:500-505, doi: 10.1097/01.tp.0000167723.46580.78.

14. van Der Hoeven JA, Ter Horst GJ, Molema G, de Vos P, Girbes AR, Postema F, et al. Effects of brain death and hemodynamic status on function and immunologic activation of the potential donor liver in the rat. Ann Surg. 2000;232:804-13, doi: 10.1097/00000658-200012000-00009.

15. Itabashi K, Ito Y, Takahashi T, Ishii K, Sato K, Kakita A. Protective effects of urinary trypsin inhibitor (UTI) on hepatic microvascular in hypotensive brain-dead rats. Eur Surg Res. 2002;34:330-8, doi: 10.1159/000063074.

16. Zhou H, Ding W, Cui X, Pan P, Zhang B, Li W. Carbon monoxide inhalation ameliorates conditions of lung grafts from brain death donors. Chin Med J (Engl). 2008;121:1411-9.

17. Urra X, Cervera A, Obach V, Climent N, Planas AM, Chamorro A. Monocytes are major players in the prognosis and risk of infection after acute stroke. Stroke. 2009;40:1262-8, doi: 10.1161/STROKEAHA.108.532085.

18. Ley K, Gaehtgens P, Fennie C, Singer MS, Lasky LA, Rosen SD. Lectin-like cell adhesion molecule1 mediates leukocyte rolling in mesenteric venules in vivo. Blood. 1991;77:2553-5.

19. Lawrence MB, Springer TA. Leukocytes roll on a selectin at physiologic flow rates: distinction from and prerequisite for adhesion through integrins. Cell. 1991;65:859-73, doi: 10.1016/0092-8674(91)90393-D.

20. von Andrian UH, Chambers JD, McEvoy LM, Bargatze RF, Arfors KE, Butcher EC. Two-step model of leukocyte-endothelial cell interaction in inflammation: distinct roles for LECAM-1 and the leukocyte beta 2 integrins in vivo. Proc Natl Acad Sci USA. 1991;88:7538-42, doi: 10.1073/pnas.88.17.7538.

21. Von Andrian UH, Hansell P, Chambers JD, Berger EM, Torres Filho I, Butcher EC et al. L-selectin functions required for beta 2-integrin-mediated neutrophil adhesion at physiological shear rates in vivo. Am J Physiol. 1992;263:H1034-44.

22. Collins T, Read MA, Neish AZ, Whitley MZ, Thanos D, Maniatis T. Transcriptional regulation of endothelial cell adhesion molecule: NF-kappa B and cytokine-inducible enhancers. FASEB J. 1995;9:899-909.

23. McHale JF, Harari OA, Marshall D, Haskard DO. Vascular endothelial cell expression of ICAM-1 and VCAM-1 at the onset of eliciting contact hypersensitivity in mice: evidence for a dominant role of TNF-alpha. J Immunol. 1999;162:1648-55.

24. Pratschke J, Wilhelm MJ, Kusaka M, Basker M, Cooper DK, Hancock WW, et al. Brain death and its influence on donor organ quality and outcome after transplantation. Transplantation. 1999;67:343-8, doi: 10.1097/00007890-199902150-00001.

25. Wilhelm MJ, Pratschke J, Laskowski IA, Paz DM, Tilney NL. Brain death and its impact on the donor heart–lessons from animal models. J Heart Lung Transplant. 2000;19:414-418, doi: 10.1016/S1053-2498(00)00073-5.

26. Webster JI, Tonelli L, Sternberg EM. Neuroendocrine regulation of immunity. Annu Rev Immunol. 2002;20:125-63, doi: 10.1146/annurev.immunol.20.082401.104914.

27. Garcia-Leme J, Farsky SP. Hormonal control of inflammatory responses. Mediators Inflamm. 1993;2:181-98, doi: 10.1155/S0962935193000250.

28. Perretti M, Ahluwalia A. The microcirculation and inflammation: site of action for glucocorticoids. Microcirculation. 2000;7:147-61, doi: 10.1111/j.1549-8719.2000.tb00117.x.

29. Tailor A, Tomlinson A, Salas A, Panés J, Granger DN, Flower RJ, et al. Dexamethasone inhibition of leucocyte adhesion to rat mesenteric postcapillary venules: role of intercellular adhesion molecule 1 and KC. Gut. 1999;45:705-12, doi: 10.1136/gut.45.5.705.

30. Mori N, Horie Y, Gerritsen ME, Anderson DC, Granger DN. Anti-inflammatory drugs and endothelial cell adhesion molecule expression in murine vascular beds. Gut. 1999;44:186-95, doi: 10.1136/gut.44.2.186.